Microelectronic Engineering 274 (2023) 111977

Contents lists available at ScienceDirect

Microelectronic Engineering

journal homepage: www.elsevier.com/locate/mee

Deep-level traps in as-grown and electron-irradiated homo-epitaxial n-GaN layers grown by MOVPE

J. Plesiewicz [a], P. Kruszewski [a,*], V.P. Markevich [b], P. Prystawko [a], S. Bulka [c], M. Hallsal [b], I. Crowe [b], L. Sun [b], A.R. Peaker [b]

[a] Institute of High Pressure Physics, Polish Academy of Sciences, Sokolowska 29/37, 01-142 Warsaw, Poland
[b] Photon Science Institute and Department of Electrical and Electronic Engineering, the University of Manchester, Manchester M13 9PL, UK
[c] Institute of Nuclear Chemistry and Technology, Dorodna 16, 03-195 Warsaw, Poland

ARTICLE INFO

Keywords:
GaN
Electron irradiation
Defects
Deep level
DLTS

ABSTRACT

The results of junction spectroscopy measurements on deep-level defects in MOVPE (Metal–Organic Vapor-Phase Epitaxy) n-GaN samples grown on highly doped Ammono-GaN and subjected to 1.5 MeV electron irradiation are compared with the published results for epi-GaN materials grown by other techniques. It is found that in addition to the commonly observed deep-level traps in n-type GaN, such as E1 (0.25 eV) and E3 (0.59 eV), 1.5-MeV electron irradiation introduces two other electron traps, EE1 and EE2, with electronic levels at about 0.14 and 0.98 eV below the conduction band edge (E_C), respectively. In the case of the EE1 level, a strong influence of the electric field (E) on the electron emission rate (e_{em}) is observed. This suggests a donor type character of this trap level. Further, we have observed that strong electric field, as high as 2×10^5 V/cm, results in lowering the activation energy of electron emission from the EE1 level down to the value of 0.095 eV. The strong $e_{em}(E)$ dependence for the EE1 trap can explain the wide variation in electronic signatures of this trap reported in previous publications. The analysis of the EE1 trap concentrations in the electron irradiated samples allowed us to estimate the average production rate of this trap by 1.5 MeV electrons as 0.125 cm^{-1} for n-GaN material grown on Ammono-GaN substrate. A series of DLTS measurements with different filling pulse lengths revealed a complexity of the EE1 trap level structure, since at least three emission signals with different capture and emission rates have been separated within the broad EE1 emission signal. Possible origins of the detected deep-level traps are discussed.

1. Introduction

Defects are present in all types of semiconductor materials and gallium nitride (GaN) is not an exception. One of the key factors that can determine the number of defects, and therefore the structural and chemical purity of an epitaxially-grown material, is the substrate used for the material growth. In nitrides, this is crucial because substrates such as sapphire, silicon, or SiC are not lattice matched and cause stress that relaxes by creating point and/or extended defects and/or dislocations [1,2]. For this reason, homoepitaxially-grown GaN-based structures are preferred for investigations of the fundamental properties and intrinsic defects in these materials. Recently, significant progress has been made in the availability of native and truly bulk GaN substrates, especially highly doped n-type substrates. In this paper, we present the results of research conducted on n-GaN layers grown on high-quality Ammono-GaN substrates ($n \sim 1 \times 10^{19}$ cm^{-3}) manufactured at the Institute of High Pressure Physics, Polish Academy of Sciences, Poland [3,4].

In the last decade, significant progress in the understanding of defects formation in GaN-based materials has been made. Numerous theoretical [5–9] and experimental papers [10–12] discussing the origin and nature of defects in GaN have been published and some important findings have been reported. As an example, based on recent HSE (Heyd-Scuseria-Ernzerhof) theoretical calculations [5,6,8,9] as well as on experimental results, an electron trap commonly observed in GaN and referred to as E3 (with an energy level at about E_c-0.58 eV) has been convincingly assigned to a Fe_{Ga} acceptor level [6,11]. On the other hand, the origin of another trap with an electronic level located at E_c-0.25 eV (E1), which is prominent and frequently reported in n-GaN, is still not well understood. However, it has been reported recently that the electric

* Corresponding author.
E-mail address: kruszew@unipress.waw.pl (P. Kruszewski).

https://doi.org/10.1016/j.mee.2023.111977
Received 1 February 2023; Received in revised form 8 March 2023; Accepted 9 March 2023
Available online 11 March 2023

field (E) significantly enhances the electron emission rate (e_{em}) for the E1 trap and the $e_{em}(E)$ dependences for this trap have been found to be characteristic of attractive traps (donor levels in n-type materials) with spherically symmetric square well potential with a radius of about 2.9 nm [12].

For studying electrically active defects, not only in GaN, junction-spectroscopy techniques such as DLTS (Deep Level Transient Spectroscopy) are frequently used [13]. In DLTS, capacitance transients due to electron emission from the trap levels present in the space charge region of tested diodes (either Schottky or p-n junctions) are measured and analyzed [13,14]. In this manner, trap levels in semiconductor materials can be studied. However, the chemical and structural identification of the traps detected in the DLTS spectra is not straightforward. For epitaxially-grown GaN, in addition to the substrate, key growth parameters such as temperature (T), pressure (P) or III/V ratio (n) are strongly correlated and any changes in these parameters can result in significant changes in the nature and concentrations of grown-in defects, which are difficult to correlate with the measured DLTS signals. One of the ways to overcome these problems is the creation of defects in a more controlled manner by electron irradiation (EI), in which for appropriately selected electron beam energy, Ga and/or N atoms can be displaced from their normal positions in the lattice creating vacancies and interstitials [15–17]. In the literature, the studies of the effects of electron irradiation and ion implantation on the formation of point defects in GaN have been intensively studied and reported [18,19], however, the majority of these works have been done on highly dislocated low-quality n-GaN materials since samples were grown mostly on sapphire [18,20–22]. Further, the results obtained for ion implanted structures are much more difficult to interpret as ions usually remain in the implanted material, often creating defects consisting of clusters of atoms complexed with other defects present in the material [23]. There are also several publications where defects created by high energy electron irradiation (5–10 MeV) were studied [19,24], however such high energy irradiation also creates complex cluster defects with rather high concentrations that significantly hinders defect analysis.

Our research is different from most other work published so far since this study was conducted on high quality GaN layers grown on native substrates (Ammono-GaN) and characterized by extremely low threading dislocation density (TDD $\sim 1 \times 10^4$ cm^{-2}) [4]. GaN layers grown on Ammono-GaN have similar TDD as in the substrate and thus the impact of threading dislocation on defects formation is minimized. Moreover, the electron irradiation process was carried out with 1.5-MeV energy ensuring experimental conditions in which simple point defects such as nitrogen vacancy (V_N), galium vacancy (V_{Ga}), nitrogen interstitial atom (N_i), and gallium interstitial atom (Ga_i) should be produced only. Finally, the paper concentrates on the results obtained for the radiation-induced EE1 electron level since a comprehensive analysis of that defect could be performed at low temperatures, which are below the temperature range in which this defect starts to annihilate [25,26]. In contrast to EE1, an analysis of the radiation-induced EE2 level is much more complicated, and for obtaining solid results more measurements on many more samples are needed. This is because the radiation-induced defects, including EE2, start to annihilate in GaN in the temperature range of 420–500 K, which overlaps with the temperature range, where the emission signal due to the EE2 trap is detected in DLTS spectra. The DLTS measurements for analysis of the EE2 trap result in the changes in the spectra due to defect annihilation/reconfiguration after each DLTS scan [10].

2. Material and methods

The samples analyzed in this study were taken from a single wafer, which was grown in a following way: first, 400-nm highly doped n$^+$-GaN layer, Si-doped to nominal value of about 2×10^{18} cm^{-3} was grown on a highly conductive n-type Ammono-GaN substrate [3,4,27]. Then, 100-nm thick silicon doped n-GaN (5×10^{17} cm^{-3}) was grown followed by 1.5-μm thick n-GaN drift layer with intended net donor concentration close to 3×10^{16} cm^{-3}. The cross-section of the wafer is shown in Fig. 1. Next, small (about 7 × 10 mm^2) samples were cut from the wafer and processed with Ni/Au Schottky diodes deposited on top surface. Ti/Al/Ni/Au ohmic contacts have been fabricated on the back side of the structure and sintered at 850 °C for 1 min in N_2 atmosphere.

The net donor concentration was determined by Capacitance – Voltage (C-V) measurements carried out at 295 K at a signal testing frequency of 1 MHz. More details of the growth and diode processing procedures can be found in one of our earlier papers [12,28].

DLTS-based measurements have been carried out within the temperature range 77 K to 500 K with an average ramping rate of 3 K/min. Capacitance transients were captured using a Boonton 72B capacitance meter (1 MHz) and MFIA (Multi Frequency Impedance Analyzer, 1-MHz), then transformed by an analog-to-digital converter and analyzed by software controlled by a computer.

Electron irradiation was performed at the Institute of Nuclear Chemistry and Technology in Warsaw, Poland. The diodes were exposed to electron energy of 1.5 MeV and irradiated with three doses/fluences: 15, 80 and 156 kGy (absorbed dose), which corresponds to 0.7, 3.7 and 7.4×10^{14} cm^{-2} exposure fluences, respectively. The irradiation was carried out at 295 K on the processed chips and the electron beam flux was directed perpendicularly to the sample surface with Ni/Au diodes faced towards the electron beam. For good heat dissipation during irradiation, the chips were mounted on a water cooled 10 cm thick copper block.

The penetration depth for 400-keV electrons in GaN is around 200 μm [10], and thus it is expected that 1.5-MeV electrons pass through the top 1.5 um thick layer of our samples without attenuation. According to the literature results [29], a homogenous distribution of radiation-induced defects has been observed alongside the 0.546 MeV electron trajectory path in GaN, therefore, a homogenous distribution of defects induced by 1.5-MeV electrons in the top GaN layer, which has been probed in our DLTS measurements, is expected.

3. Results

Fig. 2 presents conventional DLTS spectra recorded for both, reference (as-grown) material (black curve) and material irradiated with 1.5 MeV electrons to a dose of 156 kGy (red curve). The measurement parameters used for the recording of the spectrum are given in the graph. In Fig. 2, Y-axis shows the trap concentration calculated from the measured DLTS signal in accordance with the paper of Markevich et al. [12].

Two electron-emission-related peaks with their maxima at about 140 and 304 K for the DLTS rate window of 20 Hz are observed in the recorded spectrum for reference material (black curve). This spectrum resembles the DLTS spectra reported in the literature for n-GaN layers

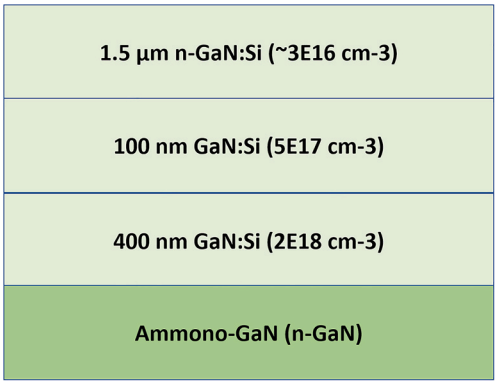

Fig. 1. The cross-section of the n-GaN wafer, samples from which have been analyzed in this study.

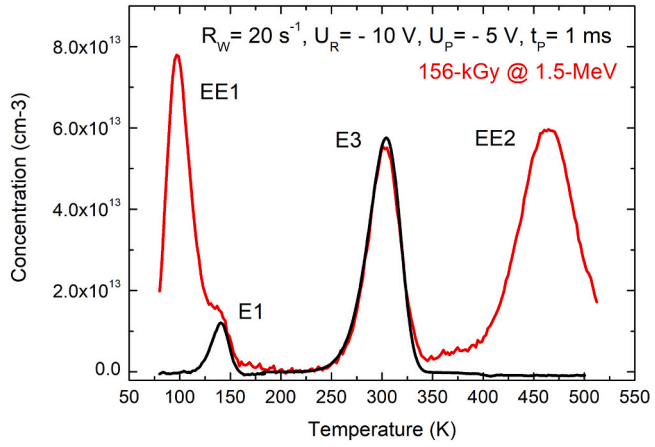

Fig. 2. Conventional DLTS spectra for both: reference sample (black curve) and 1.5 MeV electron-irradiated sample to dose of 156 kGy (red curve). (For interpretation of the references to colour in this figure legend, the reader is referred to the web version of this article.)

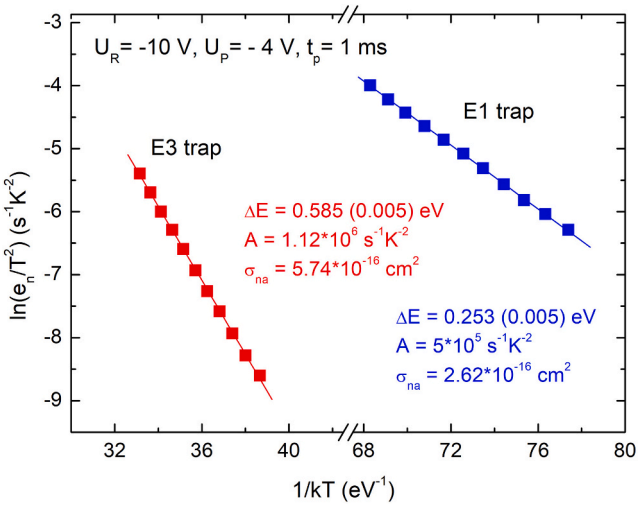

Fig. 3. Arrhenius plots of T^2-corrected electron emission rates for the E1 and E3 trap levels for a reference n-GaN sample grown on ammono-GaN. The trap signatures (ΔE, A and σ_{na}) derived from the fitting of the plots as well as the measurement parameters are given in the graph.

grown on free-standing GaN substrates [11,30,31]. The peaks in the DLTS spectrum shown in Fig. 2 for a reference sample are commonly referred to as E1 and E3 electron traps. It is worth to mention that both traps are nearly always observed in the DLTS spectra of as-grown n-type MOCVD epi-GaN irrespective of the growth parameters and substrate used for the growth [30,32–34]. Typically, E1 has lower concentration than E3 but some exceptions have been reported [12]. In addition to the commonly observed E1 and E3 traps, electron irradiation with energy of 1.5 MeV resulted in the appearance of two other electron traps, referred here as EE1 and EE2 with their maxima at about 97 and 464 K as shown in Fig. 2 (red curve), respectively. Interestingly, both electron-induced trap levels have comparable concentrations suggesting a correlation in the production of corresponding defects, such as creation of nitrogen or gallium Frenkel pairs, for example. Small changes in E1 and E3 traps concentrations, visible in Fig. 2 for the irradiated sample compared the as-grown one, are most likely due to the effect of trap concentrations inhomogeneity across the wafer rather than the effect of electron irradiation itself. Similar observations of up to two orders of magnitude variation in concentrations of the E1 and E3 trap states across the n-type epi-GaN wafers have been recently reported [11,35].

To verify the origin of the two DLTS signals with peaks located at 140 K and 304 K in the reference samples and to compare them with the similar traps reported in the literature, the electronic signatures of both traps including the activation energy for electron emission (ΔE), pre-exponential prefactor (A) and apparent capture cross-section (σ_{na}) have been obtained. This has been done using linear regression fitting of the experimental data presented in the form of Arrhenius plots as shown in Fig. 3. The measurement parameters used for the recording of the data are given in the graph. The data points shown in Fig. 3 have been obtained by the collection of Laplace DLTS spectra [36] measured at temperatures for which the rate of electron emission (e_n) from deep levels is in the range from 10 to 1000 s^{-1}. A wide range of measured e_n values for both traps allowed us to determine the activation energies with a relatively small error.

The activation energy values obtained in this manner are consistent with the literature data published for the E1 and E3 trap levels [12,30,32–34]. GaN samples irradiated with electrons have been checked with the same methodology and very close values (± 2%) have been derived confirming that the E1 and E3 traps, which present in both reference and irradiated samples, are identical and originate from the same sources.

Due to some specific limitations as discussed in the introduction section, the results and further analysis given in the paper deal mostly with the properties of the EE1 trap level. However, activation energies for both electron-induced traps have been determined and are equal to 0.14 ± 0.002 eV (Fig. 4) for EE1 and 0.98 ± 0.05 eV for EE2 (not shown in the diagram), respectively. Our low field value of ΔE for the EE1 trap and the value for the EE2 trap are in good agreement with the data reported in the literature [10,22,37].

In Fig. 4, the electric field dependent Arrhenius plots for the EE1 deep trap level in electron-irradiated n-GaN sample (156-kGy) grown on Ammono-GaN substrate are shown. The blue and black points represent experimental conditions in which Double DLTS (DDLTS) signal [13,38] for the EE1 trap level was measured in the depletion layer regions with low and high electric field values, respectively. In general, the value of the electric field in the depletion region of a diode changes linearly with the distance and reaches a maximum value at the Ni/Au-GaN interface and is zero at the point where the depletion region collapses. In our experiment, the electric field strength behaviour has been explored by sampling different parts of the depletion layer by using different value of filling pulse voltages applied to the sample as specified in Fig. 4. A

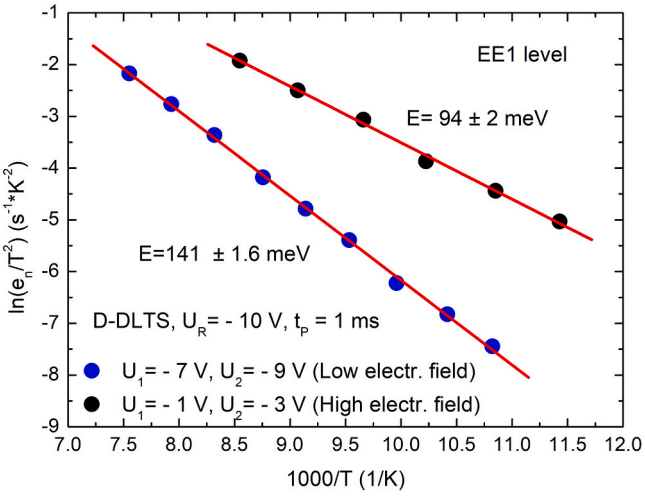

Fig. 4. Arrhenius plots of T^2-corrected electron emission rates for the EE1 deep trap level in electron-irradiated n-GaN sample grown on Ammono-GaN registered for low (5×10^4 V/cm blue points) and high (2×10^5 V/cm black points) electric field present in the space charge region, respectively. (For interpretation of the references to colour in this figure legend, the reader is referred to the web version of this article.)

comparison of emission rates and the activation energies determined from data points shown in Fig. 4 indicates that high electric field substantially enhances electron emission rate from the EE1 level, and the activation energy of electron emission obtained for that case is only $\Delta E = 0.095 \pm 0.002$ eV, while for low electric field in the depletion layer, the activation energy increases to a value of $\Delta E = 0.14 \pm 0.002$ eV. The low and high electric field strengths for the data shown in Fig. 4 are equivalent to 5×10^4 V/cm and 2×10^5 V/cm, respectively. The difference in determined activation energies for both electric fields strengths will be discussed later in the discussion section.

A family of conventional DLTS spectra measured for five different filling times (t_p), from 10 μs to 50 ms, for an electron-irradiated n-GaN sample (156 kGy) grown on Ammono-GaN substrate is shown in Fig. 5. An analysis of the changes in the DLTS spectra measured for temperatures below 220 K with measurement parameters as given in the graph shows a few of interesting effects: 1) the magnitude of the DLTS signal measured for the EE1 trap level increases significantly with the increase of the filling pulse length in the region from 10 μs to 10 ms; b) at least two or possibly three components with different temperatures at peak maxima contribute to the EE1 signal; c) Relative contributions of these components to the total emission signal due to the EE1 trap change with the filling pulse length that results in the shift of the DLTS main peak towards lower temperatures as filling pulse length increases; d) DLTS main peak saturates for times longer than 10 ms for the EE1 level, and e) the changes in magnitude of the DLTS signal for the E1 level are negligible in the range of t_p used.

The DLTS spectra measured for n-GaN samples after 1.5 MeV electron irradiation at three doses of 15, 80 and 156 kGy as well as for the non-irradiated sample (reference) are presented in Fig. 6. As expected, the DLTS signal related to the EE1 trap level increases almost linearly with the electron irradiation dose and DLTS peak maximum occur at 107 K for all three doses. In Fig. 6, small variations in magnitude of the E1 trap level signal with the peak maximum at 150 K seen for irradiated samples can be attributed to E1 trap concentration inhomogeneity across the wafer from which smaller samples were cut and then irradiated with different doses. Therefore, some local variations of E1 trap concentrations from sample to sample are possible that was previously mentioned when the DLTS results presented in Fig. 2 have been discussed. Moreover, there are no reports in the literature claiming changes in the E1 trap concentration after electron irradiation that is in agreement with our observations and interpretation.

For the devices operating in electron radiation environment, the Production Rate (PR) of traps is one of key parameters, which helps to

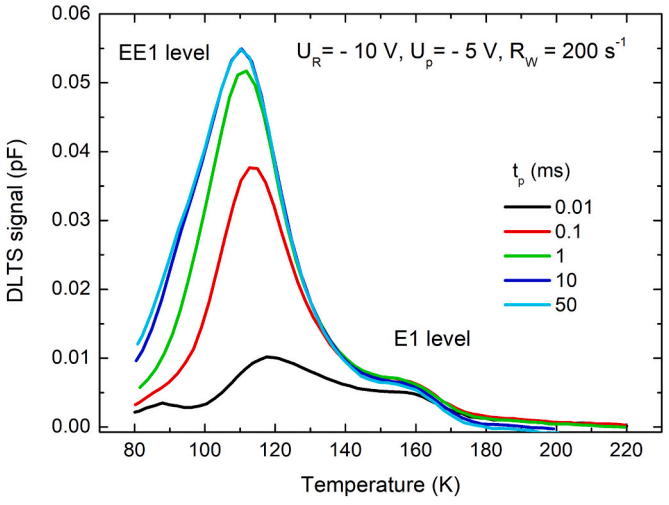

Fig. 5. A family of conventional DLTS spectra measured for five different filling pulse lengths, t_p, (from 10 μs to 50 ms) for an electron-irradiated n-GaN sample (156 kGy) grown on Ammono-GaN substrate.

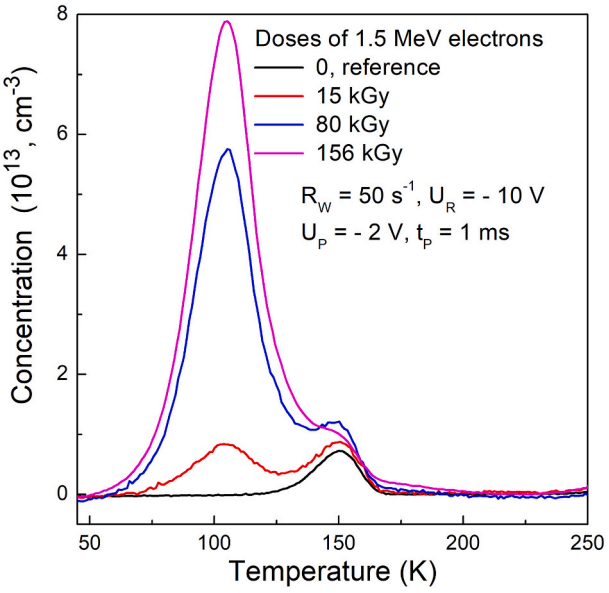

Fig. 6. A series of DLTS spectra measured for n-GaN samples after 1.5 MeV electron irradiation at doses of 15, 80 and 156 kGy, respectively. The DLTS spectrum for a non-irradiated n-GaN sample is shown in the same graph for comparison.

estimate device degradation caused by the radiation. To calculate the production rate (PR = trap concentration / incident fluence) of the EE1 trap level, which is expressed in the unit of cm^{-1}, the absorbed doses given in kGy must be recalculated to exposure fluences given in the units of cm^{-2}. In this work, the absorbed doses have been recalculated to exposure ones according to the following formula [39]:

$$D = \varnothing^* \left(\frac{Scol}{\rho}\right), \quad (1)$$

where D is the absorbed dose to medium given in Gy, Φ is the electron fluence in the medium (cm^{-2}) and $\left(\frac{S_{col}}{\rho}\right)$ is the unrestricted mass collision stopping power of the medium at the energy of the electron (in MeV*cm^2 *g^{-1} units). The mass collision stopping power was calculated using ESTAR program available at the website of the NIST (National Institute of Standards and Technology). The electron irradiation doses expressed in both units, kGy and cm^{-2}, as well as the EE1 trap concentrations and resulting production rates for the EE1 trap level are given in Table 1.

4. Discussion

The DLTS spectra and Arrhenius plots presented in Figs. 2 and 3 for the E1 and E3 trap levels in as-grown GaN samples resemble those reported by other groups for similar n-GaN layers on free standing GaN [11,30,37]. The DLTS spectrum shown in Fig. 2 for a reference sample consists of two peaks only, while for n-GaN layers grown on sapphire four or even five signals in the DLTS spectra occurred in the same

Table 1
The values of the electron irradiation doses expressed in both units (kGy and cm^{-2}), as well as the EE1 trap concentrations and resulting production rates for the EE1 trap level. The production rate was calculated as the ratio of the trap concentration to the fluence.

No.	Absorbed dose (kGy)	Exposure fluence (cm^{-2})	EE1 trap concentration (cm^{-3})	Production rate (cm^{-1})
1	15	0.7×10^{14}	0.84×10^{13}	0.12
2	80	3.7×10^{14}	5.75×10^{13}	0.15
3	156	7.4×10^{14}	7.89×10^{13}	0.11

temperature range [21,40]. This is likely due to large lattice mismatch between GaN and Al_2O_3 leading to the presence of high dislocation density (TDD ~ 10^9 cm^{-2}) and formation of dislocation-related defects. For GaN layers grown on Ammono-GaN, TDD is never higher than 5×10^5 cm^{-2} [4,27] and thus very few dislocation related defects are exptected in ovegrown GaN material.

The results obtained in our work on the E1 and E3 traps in the as-grown and and electron-irradiated GaN samples are consistent with the results and discussion on these traps reported recently by Markevich et al. [12]. Our results do not contradict the assignment of the E3 trap to an acceptor level of Fe_{Ga} [11], and the arguments that the E1 trap can be related to a donor level of a complex incorporating a native defect and an impurity atom [12,28]. However, further studies are needed for a solid identification of the E1 complex components and their locations in the lattice.

In the literature, there are no reports for electron irradiated n-GaN samples grown on Ammono-GaN, although Horita et al. [10] have studied electron irradiation induced traps in low dislocation GaN grown by HVPE on free standing GaN substrates. Here we consider in the following discussion how our results obtained mostly for the EE1 trap level are consistent with those previously reported for electron irradiated n-GaN samples.

Analysing the results published in the literature, one can notice that different groups reported different ΔE for the EE1 trap in irradiated n-GaN samples. Activation energies for electron emission from the radiation-induced trap observed in the DLTS spectra in the temperature range, which corresponds to the EE1-related signal, vary from 0.09 to 0.18 eV [10,21,20,37,41,42] with a bias that lower values have been determined for homoepitaxially grown GaN samples while higher values have been reported for samples grown on sapphire [20,21]. This trend can be related to the high concentration of dislocations in the GaN-on-sapphire material, which can act as additional sinks for the defects created by electron irradiation [18]. Furthermore, the vicinity of a dislocation can result in the movement of the energy level of the EE1 trap deeper to the bandgap. Moreover, in strained samples, such as for GaN/Al_2O_3 system, the broadening of DLTS and Laplace DLTS signals is observed, which can significantly affect the activation energies determined from Arrhenius plots of emission rates. Last but not least, the experimental conditions used for recording DLTS spectra can affect the trap paramaters such as the activation energy for emission as well. Fig. 4 presents the difference in activation energy for the EE1 level obtained for two experimental conditions: low (blue circles) and high (black circles) electric field present in the probed depletion layer of a Schottky diode, respectively. Both experimental conditions have been realized by the implementation of Double DLTS technique where fixed reverse bias and two different filling pulse voltages were used. In this approach, only a thin part of the depletion layer, with almost constant electric field, is scanned. The probing region as well as electric field strength can be easily tuned by proper selection of the filling pulse voltages [12]. The measurement parameters used in the experiment are specified in Fig. 4. As one can see (Fig. 4), the derived activation energies differ significantly for different experimental conditions and indicate that electric field enhances electron emission rate from the EE1 level. This effect is relatively strong as high electric field such as 2×10^5 V/cm (black circles) lowers the activation energy of the EE1 level down to the value of 0.095 eV. The strong enhancement of the electron emission rate by the electric field for the EE1 level suggests that the EE1 trap is associated with a donor type level [43].

Some strong arguments have been presented recently that the EE1 electron trap is related to a donor level of the nitrogen vacancy and the EE2 trap is related to an acceptor level of nitrogen interstital atom [10]. These assignments are consistent with the results of ab-initio calculations [5,44]. Our results on EE1 are, in general, consistent with the results reported by Horita et al. [10] and the results of ab-initio calculations, however, it appears that there are some unsual properties of the EE1 trap, which cannot be explained by just the occurrence of the single V_N center with a well-defined donor level close to E_c. Fig. 5 illustrates these unusual properties. It can be seen from the DLTS spectra presented in Fig. 5 that a) the EE1 emission signal consists of at least two or possibly three components, b) magnitudes of the components change with the changes in length of the filling pulse, and c) their relative contibutions vary with t_p. The observed changes cannot be explained by the presence of single species of V_N.

Among many papers dealing with the deep traps in electron irradiated GaN samples, the shape of DLTS signal related to the EE1 trap level has been analyzed in the works by Polenta et al. [20] and by Umana-Membreno et al. [42]. Polenta et al. analyzed n-GaN samples irradiated with 1-MeV electrons. The authors suggested that electron-induced DLTS peak with its maximum at 120 K and labeled as E (EE1 in this paper) consists of two deep traps, the concentrations and electronic signatures of which could be derived by a proper fitting of the recorded DLTS spectra. They found that both centers have the same thermal activation energy, 0.06 eV, however, they have different and small capture cross sections of (1–3) $\times$ 10^{-20} cm^2 and (5–8) $\times$ 10^{-19} cm^2, respectively. Moreover, the authors suggested that both traps are related to the nitrogen vacancy, but they are different complexes of V_N. In GaN, nitrogen vacancy is expected to be a donor type defect [5,44] but capture cross sections reported by Polenta et al. [20] suggest that the both traps contibuting to the *E*-trap signal are likely to be acceptor states.

Umana-Membreno et al. analyzed n-type GaN samples irradiated with gamma-rays from a ^{60}Co source [42]. In the DLTS spectra of the irradited sample they observed a radiation-induced electron emission signal in the temperature range corresponding to emission from the EE1 trap. The observed signal was labeled as G signal, and it was shown that it consist of three components, G_1, G_2, and G_3. The values of activation energies for electron emission / apparent capture cross sections were derived as 88 ± 7 meV / 2.6×10^{-18} cm^2 for G_1, 104 ± 12 meV / 1.2×10^{-18} cm^2 for G_2, and 144 ± 13 meV / 7.6×10^{-18} cm^2 for G_3. Again, the reported values of the capture cross sections are characteristic of a defect with a repulsive potential for electrons (an acceptor level in n-type semiconductor). The authors assumed that the observed radiation-induced G emission signal could be linked to the previously reported nitrogen-related defects. They mentioned further that"more complex defects may arise near the metal-GaN interface since the radiation-induced defect production rates are influenced by the presence of lattice laws and impurities" [42].

Summarising an analysis of the results reported by Polenta et al. and Umana-Membreno et al. [20,42], it should be mentioned that the authors did not take into account the effect of electric field on emission rates for the electron traps, which were observed in the DLTS spectra recorded. The net doping concentrations in the samples used in both studies were about 2.3×10^{16} cm^{-3} and 3.3×10^{16} cm^{-3}. The reverse biases used for the DLTS measurements were in the range from −2 V to −5 V, so the electric field in the probed regions of the diodes, which had the effective Schottky barrier height higher than 1 eV (as reported by Umana-Membreno et al. [42]), can reach the values higher than 2×10^5 V/cm. As shown in Fig. 4 in our paper, such *E* values can result in a significant enhancement of electron emission rates and further in reduced values of activation barriers for electron emission from the E and G traps detected by Polenta et al. [20] and Umana-Membreno et al. [42].

Our results on the EE1 trap presented in Fig. 5 are, in general consistent with the results reported by Polenta et al. and Umana-Membreno et al. [20,42]. Similarly to the previously reported results, it can be seen in Fig. 5 that the magnitude of the main DLTS peak due to the EE1 trap increases as the filling time rises and the peak maximum shifts to lower temperatures. As the filling time reaches 10 ms, DLTS signal saturates and only small changes in low temperature side of DLTS peak can be observed. The peak magnitude saturation for long filling pulses is characteristic for point-like defects in contrast to the behaviour of extended defects or clusters of dislocations, for which such a pronounced saturation does not occur [45]. We are now carrying out a

detailed study of filling pulse length dependences for different emission components of the EE1 signal, the results of which will be reported in a separate paper.

Further, we have compared the EE1 trap production rates given in Table 1 with the data reported in the literature. Fang et al. [21] reported the value of production rate of the analog of the EE1 trap for 2-MeV electron irradiation in n-GaN/Al_2O_3 as 0.2 cm^{-1}, while the value reported by Polenta et al. [20] for the case of 1-MeV electron irradiation was 0.3 cm^{-1}. In 2021, Horita et al. reported the EE1 production rate of 0.093 cm^{-1} for n-GaN/GaN samples irradiated with relatively low electron energy in the range of 100–400 keV [10].

The EE1 production rates obtained within this study vary slightly from sample to sample and have been estimated as 0.12, 0.15, and 0.11 cm^{-1}, in order of increasing exposure fluences (Table 1). Since our samples have been irradiated with 1.5-MeV electrons, a direct comparison to reported PRs is difficult but the derived production rates are in quite good agreement with other experimentally determined values [10,20,21]. The EE1 PR values obtained for our GaN samples seem to be reasonable but, in our opinion, should be slightly larger ~0.2–0.4 cm^{-1} as it was theoretically predicted from non-ionizing energy loss (NIEL) calculations and recently obtained by Aoshima [46]. We think that this is due to the fact that exposure fluences converted from absorbed doses and measured for a reference material, alanine, given in kGy seems to be slightly underestimated.

5. Conclusions

The results of DLTS and Laplace DLTS measurements on MOVPE n-GaN samples grown on highly doped Ammono-GaN and subjected to 1.5 MeV electron irradiation are presented and compared with the published results for epi-GaN materials grown by other techniques. We have shown that besides commonly observed deep levels in n-type GaN, such as E1 (0.25 eV) and E3 (0.59 eV), 1.5-MeV electron irradiation introduces two other electron traps, EE1 (0.14 eV) and EE2 (0.98 eV), respectively. Our results on the E3 trap are consistent with the results reported in literature for this trap and do not contradict with its recent assignment to an acceptor level of Fe_{Ga} [11]. The origin of the E1 trap is still not certain [12,28], and in the present work we have not obtained any solid results for its elucidation.

Regarding the electron-irradiation-induced EE1 trap, we have observed strong influence of the electric field on the electron emission rate for this trap, which has not been mentioned in the previous publications. This result indicates a donor type character of this trap level that is consistent with the suggested assignment of the trap to a donor level of nitrogen vacancy [5,10,44]. Further, we have observed that strong electric field as high as 2×10^5 V/cm can lower the effective activation energy of electron emission from the EE1 level down to the value of 0.095 eV. The strong $e_{em}(E)$ dependence for the EE1 trap can explain the wide variation in electronic signatures of this trap reported in previous publications. Furthermore, a series of DLTS measurements carried out with different filling pulse lengths has revealed a complexity of the EE1 trap level structure, since up to three emission signals with different capture and emission rates can be separated within the broad EE1 emission signal. Apparently, our results and results reported previously on the EE1 trap [20,42] indicate that there are some unsual properties of the EE1 trap, which cannot be explained by its assignment to the single V_N center with a well-defined donor level close to E_c. A further study is neccessary for the separation and characterization of the three detected components of the EE1 trap and elucidation their possible origins, which is in progress at the moment.

Finally, the analysis of the total EE1 trap concentrations in the electron irradiated samples allowed us to estimate the average production rate of this trap by 1.5 MeV electrons as 0.125 cm^{-1} for n-GaN material grown on Ammono-GaN substrate. Importantly, there are no papers in the literature, which report production rates of the electron-irradiation-induced defects in n-GaN material grown on Ammono-GaN substrate, and we fill this gap in our work.

Credit author statement

J. Plesiewicz: Investigation, Formal analysis **P. Kruszewski**: Conceptualization, Investigation, Formal analysis, Visualization, Writing - Original Draft, Review & Editing **V. P. Markevich**: Investigation, Formal analysis, Writing, Review & Editing **P. Prystawko**: Resources, Investigation **S. Bulka**: Investigation **M. Hallsal:** Editing **I. Crowe**: Editing L. **Sun**: Editing **A. R. Peaker**: Supervision, Writing - Review & Editing.

Declaration of Competing Interest

The authors declare no conflict of interest.

Data availability

The data that support the findings of this study are available from the corresponding author upon reasonable request.

Acknowledgement

The authors would like to thank Dr. George T Nelson (AIM Photonics - American Institute for Manufacturing Integrated Photonic, Rochester, USA) for a freeware software dedicated for DLTS data collection and further processing (https://github.com/nelsongt/mfiaDLTS) and compatible with MFLI lock-in amplifier developed by Zurich Instruments.

The work in the UK was funded by EPSRC via grant EP/TO25131/1. Polish authors would like to thank the National Science Centre, Poland, for financial support through Projects No. 2020/37/B/ST5/02593 and No. 2019/33/B/ST5/02756.

Referencees

[1] J.S. Speck, S.J. Rosner, Physica B 273–274 (1999) 24–32, https://doi.org/10.1016/S0921-4526(99)00399-3.
[2] M.A. Moram, C.S. Ghedia, D.V.S. Rao, J.S. Barnard, Y. Zhang, M.J. Kappers, C. J. Humphreys, J. Appl. Phys. 106 (2009), 073513, https://doi.org/10.1063/1.3225920.
[3] M. Zajac, R. Kucharski, K. Grabianska, A. Gwardys-Bak, A. Puchalski, D. Wasik, E. Litwin-Staszewska, R. Piotrzkowski, J.Z. Domagala, M. Bockowski, Prog. Cryst. Growth Charact. Mater. 64 (2018) 63–74, https://doi.org/10.1016/j.pcrysgrow.2018.05.001.
[4] R. Kucharski, M. Zajac, R. Doradzinski, M. Rudzinski, R. Kudrawiec, R. Dwilinski, Semicond. Sci. Technol. 27 (2012), 024007, https://doi.org/10.1088/0268-1242/27/2/024007.
[5] J.L. Lyons, C.G. Van de Walle, npj Comput. Mater. 3 (2017) 12, https://doi.org/10.1038/s41524-017-0014-2.
[6] D. Wickramaratne, J.X. Shen, C.E. Dreyer, A. Alkauskas, C.G. Van de Walle, Phys. Rev. B 99 (2019), 205202, https://doi.org/10.1103/PhysRevB.99.205202.
[7] Y.S. Puzyrev, R.D. Schrimpf, D.M. Fleetwood, S.T. Pantelides, Appl. Phys. Lett. 106 (2015), 053505, https://doi.org/10.1063/1.4907675.
[8] M. Matsubara, E. Bellotti, J. Appl. Phys. 121 (2017), 195701, https://doi.org/10.1063/1.4983452.
[9] M. Matsubara, E. Bellotti, J. Appl. Phys. 121 (2017), 195702, https://doi.org/10.1063/1.4983453.
[10] M. Horita, T. Narita, T. Kachi, J. Suda, Appl. Phys. Lett. 118 (2021), 012106, https://doi.org/10.1063/5.0035235.
[11] M. Horita, T. Narita, T. Kachi, J. Suda, Appl. Phys. Express 13 (2020), 071007, https://doi.org/10.35848/1882-0786/ab9e7c.
[12] V.P. Markevich, M.P. Halsall, L. Sun, I.F. Crowe, A.R. Peaker, P. Kruszewski, J. Plesiewicz, P. Prystawko, S. Bulka, R. Jakiela, Phys. Status Solidi B (2023) 2200545, https://doi.org/10.1002/pssb.202200545.
[13] A.R. Peaker, V.P. Markevich, J. Coutinho, J. Appl. Phys. 123 (2018), 161559, https://doi.org/10.1063/1.5011327.
[14] D.V. Lang, J. Appl. Phys. 45 (1974) 3023–3032, https://doi.org/10.1063/1.1663719.
[15] J. Nord, K. Nordlund, J. Keinonen, K. Albe, Nucl. Instrum. Methods Phys. Res., Sect. B 202 (2003) 93–99, https://doi.org/10.1016/S0168-583X(02)01839-6.
[16] H.Y. Xiao, F. Gao, X.T. Zu, W.J. Weber, J. Appl. Phys. 105 (2009), 123527, https://doi.org/10.1063/1.3153277.

[17] D.C. Look, D.C. Reynolds, J.W. Hemsky, J.R. Sizelove, R.L. Jones, R.J. Molnar, Phys. Rev. Lett. 79 (1997) 2273–2276, https://doi.org/10.1103/PhysRevLett.79.2273.
[18] S.J. Pearton, R. Deist, F. Ren, L. Liu, A.Y. Polyakov, J. Kim, J. Vac. Sci. Technol. A 31 (2013), 050801, https://doi.org/10.1116/1.4799504.
[19] A.Y. Polyakov, S.J. Pearton, P. Frenzer, F. Ren, L. Liu, J. Kim, J. Mater. Chem. C 1 (2013) 877–887, https://doi.org/10.1039/C2TC00039C.
[20] L. Polenta, Z.-Q. Fang, D.C. Look, Appl. Phys. Lett. 76 (2000) 2086–2088, https://doi.org/10.1063/1.126263.
[21] Z.Q. Fang, J.W. Hemsky, D.C. Look, M.P. Mack, Appl. Phys. Lett. 72 (1998) 448–449, https://doi.org/10.1063/1.120783.
[22] D.C. Look, Phys. Status Solidi B 228 (2001) 293–302, https://doi.org/10.1002/1521-3951(200111)228:1 < 293::AID-PSSB293 > 3.0.CO;2-F.
[23] Semiconductors and Semimetals, Defects in Semiconductors, Edited by Lucia Romano, Vittorio Privitera, Chennupati Jagadish, Elsevier, ISBN: 978–0–12-801,935-1, Elsevier, 2015.
[24] K. Lorenz, J.G. Marques, N. Franco, E. Alves, M. Peres, M.R. Correia, T. Monteiro, Nucl. Instrum. Meth. B 266 (2008) 2780, https://doi.org/10.1116/1.4799504.
[25] K. Saarinen, T. Suski, I. Grzegory, D.C. Look, Phys. Rev. B 64 (2001), 233201, https://doi.org/10.1103/PhysRevB.64.233201.
[26] G. Alfieri, V.K. Sundaramoorthy, R. Micheletto, J. Appl. Phys. 123 (2018), 205303, https://doi.org/10.1063/1.5029254.
[27] R. Dwilinski, R. Doradzinski, J. Garczynski, L.P. Sierzputowski, A. Puchalski, Y. Kanbara, K. Yagi, H. Minakuch, H. Hayash, J. Cryst. Growth 310 (2008) 3911–3916, https://doi.org/10.1016/j.jcrysgro.2008.06.036.
[28] P. Kruszewski, P. Kaminski, R. Kozlowski, J. Zelazko, R. Czernecki, M. Leszczynski, A. Turos, Semicond. Sci. Technol. 36 (2021), 035014, https://doi.org/10.1088/1361-6641/abe317.
[29] S.A. Goodman, F.D. Auret, M.J. Legodi, B. Beaumont, P. Gibart, Appl. Phys. Lett. 78 (2001) 3815–3817, https://doi.org/10.1063/1.1379057.
[30] Y. Tokuda, ECS Trans. 75 (2016) 39, https://doi.org/10.1149/07504.0039ecst.
[31] T. Tanaka, K. Shiojima, T. Mishima, Y. Tokuda, Jpn. J. Appl. Phys. 55 (2016), 061101, https://doi.org/10.7567/JJAP.55.061101.
[32] C.D. Wang, L.S. Yu, S.S. Lau, E.T. Yu, W. Kim, A.E. Botchkarev, H. Morkoc, Appl. Phys. Lett. 72 (1998) 1211–1213, https://doi.org/10.1063/1.121016.
[33] P. Hacke, T. Detchprohm, K. Hiramatsu, N. Sawaki, J. Appl. Phys. 76 (1994) 304–309, https://doi.org/10.1063/1.357144.
[34] D. Johnstone, S. Biyikli, S. Dogan, Y.T. Moon, F. Yun, H. Morkoc, Proc. SPIE 5739 (2005), https://doi.org/10.1117/12.591047.
[35] P. Kruszewski, J. Plesiewicz, P. Prystawko, E. Grzanka, L. Marona, Acta Phys. Pol. A 142 (2022) 611, https://doi.org/10.12693/APhysPolA.142.611.
[36] L. Dobaczewski, P. Kaczor, I.D. Hawkins, A.R.J. Peaker, J. Appl. Phys. 76 (1994) 194–198, https://doi.org/10.1063/1.357126.
[37] T.T. Duc, G. Pozina, N.T. Son, O. Kordina, E. Janzén, T. Ohshima, C. Hemmingsson, J. Appl. Phys. 119 (2016), 095707, https://doi.org/10.1063/1.4943029.
[38] H. Lefevre, M. Schulz, Appl. Phys. 12 (1977) 45–53, https://doi.org/10.1007/BF00900067.
[39] J.P. Seuntjens, W. Strydom, K.R. Podgorsak, Review of Radiation Oncology Physics: A Handbook for Teachers and Students, International Atomic Energy Agency (IAEA), Austria, May 2003. ISBN: 9201073046.
[40] Z.Q. Fang, L. Polenta, J.W. Hemsky, D.C. Look, International Semiconducting and Insulating Materials Conference, SIMC-XI (Cat. No.00CH37046), Canberra, ACT, Australia, 2000, pp. 35–42, https://doi.org/10.1109/SIM.2000.939193.
[41] K. Aoshima, K. Kanegae, M. Horita, J. Suda, AIP Adv. 10 (2020), 045023, https://doi.org/10.1063/1.5144158.
[42] G.A. Umana-Membreno, J.M. Dell, G. Parish, B.D. Nener, L. Faraone, U.K. Mishra, IEEE Trans. Electr. Dev. 50 (2003) 2326–2334, https://doi.org/10.1109/TED.2003.820122.
[43] S.D. Ganichev, E. Ziemann, W. Prittl, I.N. Yassievich, A.A. Istratov, E.R. Weber, Phys. Rev. B - Condens. Matter Mater. Phys. 61 (2000) 10361–10365, https://doi.org/10.1103/PhysRevB.61.10361.
[44] J.L. Lyons, D. Wickramaratne, C.G. Van de Walle, J. Appl. Phys. 129 (2021), 111101, https://doi.org/10.1063/5.0041506.
[45] D. Cavalcoli, A. Cavallini, E. Gombia, Phys. Rev. B 56 (1997) 10208–10214, https://doi.org/10.1103/PhysRevB.56.10208.
[46] K. Aoshima, M. Horita, J. Suda, Appl. Phys. Lett. 122 (2023), 012106, https://doi.org/10.1063/5.0128709.